V European Conference on Computational Fluid Dynamics
ECCOMAS CFD 2010
J. C. F. Pereira and A. Sequeira (Eds)
Lisbon, Portugal,14-17 June 2010

NUMERICAL MODELLING OF WAVE-STRUCTURE INTERACTION WITH A THREE DIMENSIONAL NAVIER-STOKES MODEL

Lara, J. L.*, Losada I. J.*, del Jesus, M.*, Barajas, G.* and Guanche R.*

*Environmental Hydraulics Institute "IH Cantabria",
Universidad de Cantabria,
E.T.S.I. de Caminos, Canales y Puertos
Avda. de los Castros s/n
39005, Santander, Spain
e-mail: lopezjav@unican.es

Key words: wave-structure interaction, porous media flow, VOF method

Abstract. *This paper describes the capability of a new model, called IH-3VOF to simulate wave-structure interaction problems using a three-dimensional approach. The model is able to deal with physical processes associated with wave interaction with porous structures. The model considers the VARANS equations, a volume-averaged version of the traditional RANS (Reynolds Averaged Navier-Stokes) equations. Turbulence is modeled using a k-ϵ approach, not only at the clear fluid region but also inside the porous media. The model has been validated in two cases. First, time evolution of free surface displacement at a fish tank including a porous dam has been computed. Numerical simulations were calibrated by adjusting the porous flow empirical coefficients for two granular material characteristics. The model is proven to reproduce with a high degree of agreement the free surface evolution during the seeping process. Porous flow parameters have been found different for both materials as expected because of the difference in the Reynolds number and are in agreement with previous literature. Simulations of a solitary wave interaction with an overtopped structure are presented, showing the excellent performance of the model in reproducing wave induced pattern around the structure. The model is proven to be a powerful tool in examining the near-field flow characteristics around porous structures.*

1 INTRODUCTION

Design conditions for coastal structures should include a correct assessment of the structure functional response. The most relevant hydraulic processes to be considered at wave-structure interaction encompass wave reflection, wave dissipation, wave transmission resulting from wave overtopping and wave penetration through the porous structures, wave diffraction, run-up and wave breaking, involving several time and length scales, such as gravity waves ($\sim$ 100 m, $\sim$ 10 s) or turbulent motions ($<$1 s, $\sim 10^{-3}$ m).

Traditionally wave-structure interaction has been studied through physical tests (two- and three-dimensional), especially small-scale model tests. Empirical formulations arisen from physical modeling present several restrictions, among which a relatively narrow range of applicability. Many other issues related with scale factors or processes such as porous media flow, wave impacts or viscous effects are not correctly represented in the experiments. A great effort has been made over the last decade in the numerical modeling of wave interaction with coastal structures to overcome these limitations. Several approaches have been followed to study coastal structure induced hydrodynamics. Among other existing approaches, Nonlinear Shallow Water (NSW), Boussinesq-type or Navier-Stokes equations models have traditionally been used.

Although good results in terms of averaged magnitudes have been obtained using NSW equation[1,2], vertical velocity structure can not be resolved using this approach. Moreover, the energy transfer to higher frequencies occurring before wave breaking cannot be reproduced accurately due to the lack of dispersion. Besides porous media flow is not directly solved, and has to be included in the momentum equation through an empirical friction term.

Boussinesq-type models are able to include frequency dispersion, a depth-dependent velocity profile, and can be applied to both breaking and non-breaking waves. A great effort has been devoted in order to relax the original equations by deriving the extended Boussinesq equations[3]. However, this type of models requires setting both the triggering wave breaking mechanism and the subsequent wave energy dissipation due to wave breaking. These models fail to reproduce the strong nonlinear shoaling prior to wave breaking and the free-surface and velocity higher order statistics which are thought to be relevant for structure stability. Based on Boussinesq equation wave interaction with porous structures has been modelled in the absence of breaking[4].

Navier-Stokes equations models have been incorporated in the last decade to the study of wave-strucure interaction problems. The number of simplifying assumptions assumed in the equations is lower than in other approaches. These models are able to calculate flows in complex geometries and provide very refined information on the velocity, pressure and turbulence field.

Models based on a two dimensional eulerian Navier-Stokes set of equations[5,6,7] have proven to be powerful to address wave-induced processes. Moreover, wave flow within the porous media can be simulated. Stability (i.e.: wave induced loads) or functionality

(i.e.: wave reflection or overtopping) have been reproduced numerically with a high degree of accuracy, introducing new models to be used as a complementary tool in the design process. However, the range of applicability of these results is limited to normal wave incidence.

Three dimensional wave-induced processes such as wave radiation and diffraction around breakwater trunks and heads or oblique wave incidence can only be studied based on a three dimensional approach. SPH (Smoothed Particle Hydrodynamics) has recently been applied to coastal engineering. This approach solves the flow from the Lagrangian point of view, calculating the kinematics of each particle and its interaction with neighbour particles. The Lagrangian nature of SPH makes it well suited to simulate free surface flows with rapid changes of the flow field. However, SPH models are very expensive from the computational point of view and they cannot be applied to solve the large domains that wave-structure interaction requires. Recently[8] it has been presented a two dimensional model which takes into account wave interaction with a porous flow structure.

Several approaches based on the use of Eulerian three dimensional Navier-Stokes set of equations can be found in literature[9,10,11,12]. However, none of them are able to solve porous media flow therefore coastal structures are treated as impermeable. In this work, a new three dimensional Navier-Stokes model, called IH-3VOF is presented. A new set of equations has been derived to include porous media flow in the equations.

The paper is organized as follows. In the next section, the numerical model is presented including the mathematical description and the numerical implementation. The porous flow calibration-validation is presented next for a classic dam-break problem. Finally, the hydrodynamics induced by a solitary wave impinging on a box is described. Some conclusions are closing the paper.

2 NUMERICAL MODEL DESCRIPTION

The present study uses the IH-3VOF model, whose main features are described in this section. IH-3VOF is based on TRUCHAS model developed at Los Alamos National Laboratory, which solves three dimensional Navier–Stokes equations for a multi-phase transient flow. Free surface is tracked with the volume-of-fluid technique (VOF)[13]. IH-3VOF extends TRUCHAS model applicability by solving flow in porous media with the VARANS equations and a k-ϵ turbulence model. Moreover surface gravity waves can be generated. All that features make IH-3VOF a tool to deal specially with coastal engineering issues. In this section mathematical formulation is presented first. Numerical implementation details are given next.

2.1 Mathematical formulation

The IH-3VOF model solves the three dimensional Reynolds Averaged Navier-Stokes (RANS) equations, based on the decomposition of the instantaneous velocity and pressure fields into mean and turbulent components. Reynolds stresses are closed with a k-ϵ

turbulence model.

The direct resolution of the flow field inside the porous media is not affordable, given the complex structure of porous materials. In practice, rubble mound coastal structures are made of individual stones or armour units with a random geometry. Moreover, to solve the flow characteristics inside the gaps implies a very fine grid increasing the computational cost. To overcome these limitations, flow within the porous media is then volume averaged in a control volume larger than the pore structure but smaller than the characteristic length scale of the flow. The following spatial average operator is introduced and applied to the RANS equation:

$$VA(\alpha) = \langle \alpha \rangle^f = \frac{1}{V_f} \int_{V_f} \alpha \ dV \tag{1}$$

where the subscript f means intrinsic magnitude. Intrinsic magnitudes can be related with averaged magnitudes (also called Darcy's magnitudes) with: $\langle a \rangle = n \langle a \rangle^f$ where n is the porosity and is defined as: $n = \frac{V_f}{V}$.

Applying this operator implies the Reynolds averaged magnitudes are split into a mean spatial averaged quantity and a spatial fluctuation part as follows:

$$\bar{\alpha} = \langle \bar{\alpha} \rangle + \alpha'' \tag{2}$$

It is important to note that this operation transforms a porous media made of a solid skeleton and gaps into a continuous and homogeneous medium, characterized by material properties such as porosity or nominal diameter. Once this operator is applied small scale spatial fluctuations disappear from the solution, and then the small details of the pore channel geometry are no more needed in order to obtain solutions.

Introducing now the decomposition given in (2) into the RANS equations, the volume-averaged Reynolds-averaged Navier–Stokes equations (VARANS) are obtained,

$$\frac{\partial \langle \bar{u} \rangle_i^f}{\partial t} + \langle \bar{u} \rangle_j^f \frac{\partial \langle \bar{u} \rangle_i^f}{\partial x_j} = -\frac{1}{\rho} \frac{\partial \langle \bar{p} \rangle^f}{\partial x_i} + g_i + \frac{\partial}{\partial x_j} \left(\nu \frac{\partial \langle \bar{u} \rangle_i^f}{\partial x_j} \right)$$

$$- \left\langle \frac{\partial \overline{u_i' u_j'}}{\partial x_j} \right\rangle^f - \left\langle \frac{\partial (u_i'' u_j'')}{\partial x_j} \right\rangle^f + \frac{1}{V_f} \int_{\partial V_s} \left(\frac{1}{\rho} \bar{p} + \nu \frac{\partial \bar{u}_i}{\partial x_j} \right) \mathbf{n} dA \tag{3}$$

and also the mass conservation equation for the volume-averaged ensemble-averaged variables:

$$\frac{\partial \langle \bar{u} \rangle_i^f}{\partial x_i} = 0 \tag{4}$$

It can be readily seen that mass conservation preserves its expression but changing the instantaneous variable with the ensemble-averaged velocity or with the volume-averaged ensemble-averaged velocity. However, at each averaging operation applied to the momentum conservation equation, new terms appear that need to be modeled in order to obtain accurate solutions (see second line in equation (3)).

The first of these terms is the volume-averaging Reynolds stress-tensor while the last two terms correspond with the effects that the porous medium causes to the flow. These two terms need closure equations to model the behaviour of the processes by them represented. This closure model is known as the Forchheimer equation and can be expressed as,

$$-\left\langle \frac{\partial(u_i'' u_j'')}{\partial x_j} \right\rangle^f + \frac{1}{V_f}\int_{\partial V_s}\left(\frac{1}{\rho}\bar{p} + \nu\frac{\partial \bar{u}_i}{\partial x_j}\right)\mathbf{n}dA =$$

$$-\left[\frac{\alpha\nu(1-n)^2}{n^2 D_{50}^2}\langle\bar{u}_i\rangle + \frac{\beta(1-n)}{nD_{50}}\langle\bar{u}_i\rangle \parallel \langle\bar{u}_i\rangle \parallel + c_A\frac{\partial\langle\bar{u}_i\rangle}{\partial t}\right] \tag{5}$$

where c_A is the added mass coefficient and α and β two empirical coefficients associated with the linear and nonlinear drag force respectively. The third term of the right-hand side of equation accounts for the inertial effect. The precise descriptions of the c_A, α and β coefficients are still not fully understood. They depend a priori on the pore Reynolds number and flow directions.

In order to close the VARANS equations (3) a two equation turbulence model may be used. IH-3VOF makes use of a k-ϵ model. In order to also consider the volume averaging within the porous media, the k-ϵ equations need to be transformed, yielding the form presented in the following equations:

$$\begin{aligned}\rho\left[\frac{\partial\langle k\rangle^f}{\partial t} + \langle\bar{u}_j\rangle^f\frac{\partial\langle k\rangle^f}{\partial x_j}\right] &= \langle\tau_{ij}\rangle^f\langle S_{ij}\rangle^f - \rho\langle\epsilon\rangle^f + \\ &\frac{\partial}{\partial x_j}\left[\left(\mu + \frac{\langle\mu_T\rangle^f}{\sigma_k}\right)\frac{\partial\langle k\rangle^f}{\partial x_j}\right] + \epsilon_\infty\end{aligned} \tag{6}$$

$$\begin{aligned}\rho\left[\frac{\langle\epsilon\rangle^f}{\partial t} + \langle\bar{u}_j\rangle^f\frac{\partial\langle\epsilon\rangle^f}{\partial x_j}\right] &= C_{\epsilon1}\frac{\langle\epsilon\rangle^f}{\langle k\rangle^f}\langle\widetilde{\tau_{ij}}\rangle^f\langle S_{ij}\rangle^f + C_{\epsilon2}\rho\frac{(\langle\epsilon\rangle^f)^2}{\langle k\rangle^f} + \\ &\frac{\partial}{\partial x_j}\left[\left(\mu + \frac{\langle\mu_T\rangle^f}{\sigma_k}\right)\frac{\partial\langle\epsilon\rangle^f}{\partial x_j}\right] + C_{\epsilon2}\frac{\epsilon_\infty^2}{k_\infty}\end{aligned} \tag{7}$$

It can be shown that during volume averaging of the turbulence model new terms appear which represent the effect of spatial averaging (last terms in equations (6) and (7)). These terms model the turbulence production and dissipation that occurs inside the averaging volume which is filtered out in the averaging process. Modelling proposed by Nakayama and Kuwahara[21] are considered as follows:

$$k_\infty = 3.7\frac{1-\Phi}{\sqrt{\Phi}} \parallel \langle\bar{u}_i\rangle \parallel^2 \tag{8}$$

$$\epsilon_\infty = 39\frac{(1-\Phi)^2}{\Phi}\frac{\parallel \langle\bar{u}_i\rangle \parallel^3}{H} \tag{9}$$

IH-3VOF uses the VOF (Volume of Fluid) technique to track the free surface evolution[13]. The algorithm is based upon a well-defined, second-order geometric solution of a volume evolution equation. The method utilizes local discrete material volume and velocity data to track interfaces of arbitrarily complex topology. A linearity preserving, piecewise linear interface geometry approximation ensures that solutions generated retain second-order spatial accuracy. This point is crucial in terms of an accurate reproduction of the free surface evolution in complex geometries such as wave breaking.

2.2 Numerical implementation

Equations are discretized in IH-3VOF model following the finite volume technique. A collocated grid is considered in order to define magnitudes. Both structures and unstructured meshes can be considered. To suppress spatial oscillations in the pressure and velocity, the well known Rhie-Chow method is applied. Parallel computation techniques are used to speed up simulations. Chaco software (Sandia National Laboratory) is used to perform domain subdivision. Chaco does not account for the physical characteristics of the various regions of the mesh, only the connectivity of the mesh.

A two step fractional method is considered to solve velocity and pressure field. Resulting Poisson equation is solved with the FGMRES (generalized minimal residual) method.

3 FLOW IN POROUS MEDIA

The use of the numerical model as a predictive tool for wave-porous structure interaction requires the previous calibration of the numerical parameters governing the hydrodynamics of the system. Although several works can be found in literature for several modeling approaches, calibration is needed for the new set of equations presented here. Experiments carried out by Lin[14] are presented first. Numerical set-up is discussed next. Calibration and validation work results are shown in the following sections.

3.1 Experiments description

In order to validate the model, experiments carried out by Lin[14] are used. The main reason for choosing these experiments among other existing in the literature is because they provide free surface evolution in both porous media and clear fluid. The fluid interaction with the porous structure and its evolution in time is achieved in detail.

Lin[14] recorded flow passing through a porous dam in a fish tank, using two types of granular material: crushed stones and glass beads. Nominal diameter and porosity were 1.59 cm and 0.49 for crushed stones and 0.30 cm and 0.39 for glass beads, respectively. The fish tank was 89.2 cm long, 44 cm wide and 58 cm high. The porous dam, placed at the middle of the tank, was 29 cm long, 44 cm wide (it occupies the whole fish tank width) and high enough to ensure that water never reached its upper edge. Water was initially confined in a reservoir between one side of the tank and a gate 2 cm away from the porous dam (see figure 1). Three water elevations of the initial reservoir were considered

for both granular material characteristics: 35 cm, 25 cm and 15 cm. At the beginning of the experiments, the gate was opened and the water was released interacting with the porous material and percolating into the dry area. Water motion though the porous dam and the clear fluid areas was recorded by a camera. Further details about the experiments can be found in Lin[14].

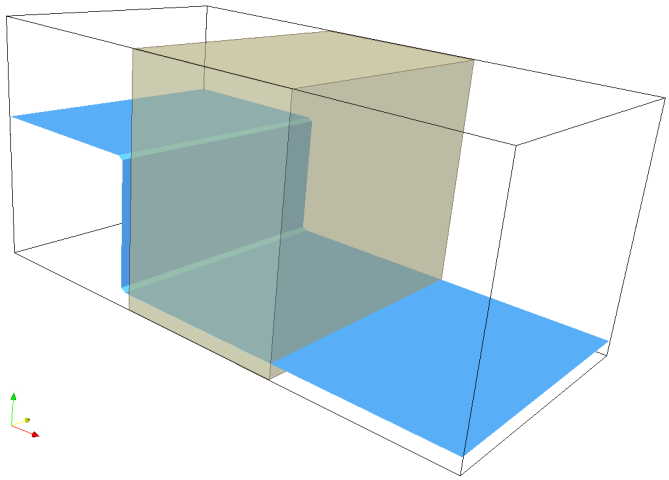

Figure 1: Initial stage for the porous dam breaking.

3.2 Computational domain

The numerical wave tank was designed as close as possible to the experimental set-up. Different discretizations were used in order to investigate the cell size dependence on the numerical solutions and also to evaluate the computational cost. Two uniform grids were considered. The cell size was 1x1x0.5 cm ($\Delta x/\Delta y/\Delta z$) and 0.5x0.5x0.25 cm ($\Delta x/\Delta y/\Delta z$) for the coarser and the finer grid respectively.

Figure 2 shows the influence of the cell size in the numerical computations for the medium water elevation at the initial reservoir for crushed stones dam. Laboratory data are presented in circles. Coarse and fine grid calculations are presented in dashed black line and solid gray line respectively.

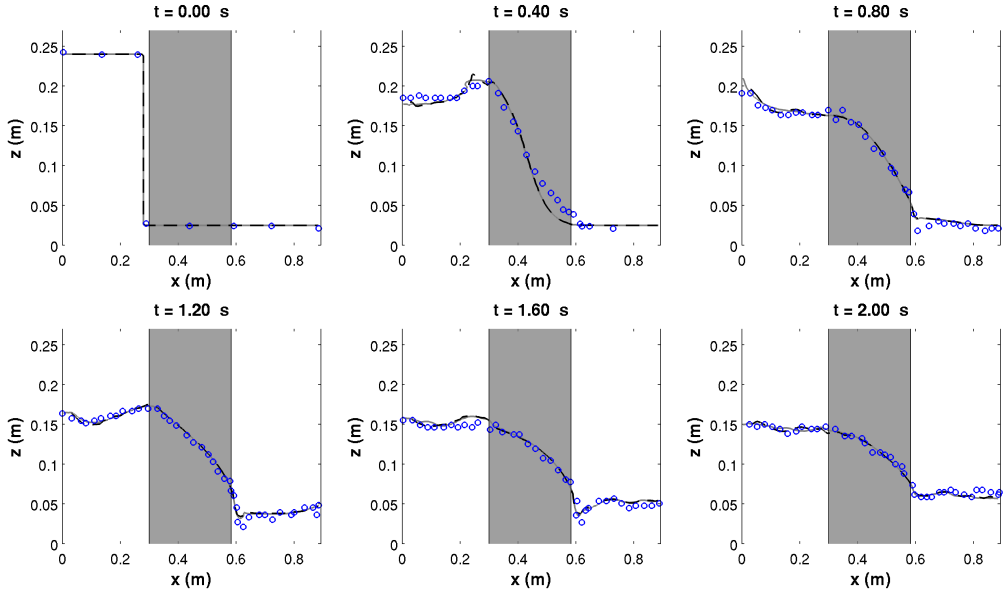

Figure 2: Grid size influence: laboratory data (circles), coarse grid (dashed black line) and fine (solid gray line).

As can be observed in the figures, both numerical simulations show almost the same results. When water rushes to the dam some reflected wave at the left side part of the porous dam is created, generating small amplitude bore (see t=0.4 s panel) which is better defined by the finer grid size. Similar behavior is observed at t=0.8 s stage when the reflected wave reaches the fish tank wall. No significant differences are observed when water is seeped out of the dam at its right side.

According to the presented results and also because of the larger computational cost observed for the finer grid, the coarser grid was used for this study.

3.3 Numerical model calibration

As previously explained, the flow field in the porous media is described in the IH-3VOF model by volume-averaging the RANS equations. The process of volume-averaging leads to the introduction in the momentum equation of two unclosed terms which are modelled collectively using the Forchheimer's relationship as presented by Hsu[15].

The expression used in the model for the linear and nonlinear drag forces is given by,

$$I = \frac{\alpha\nu(1-n)^2}{n^2 D_{50}^2}\vec{u} + \frac{\beta(1-n)}{n^2 D_{50}}\vec{u}|\vec{u}| \tag{10}$$

where I is the hydraulic gradient and α and β are the only two empirical parameters

used in the calibration of the numerical model, n is the porosity, ν the kinematic viscosity and $\vec{u}$ stands for velocity. An additional parameter, c_A affecting the inertia term is included in the formulation to take into account the added mass.

The precise descriptions of the α and β coefficients are still not fully understood for oscillatory flows. They depend on several parameters such as the Reynolds number, the shape of the stones, the grade of the porous material, the permeability and of course the flow characteristics. Several researchers have suggested different values[16,17]. However, when comparing different formulations, attention has to be paid to the fact that discrepancies may exist in the expressions of the terms and that parameter values change depending on the flow conditions. Based on previous works focused on a two dimensional RANS modeling[18,19,20,5,7] we have experienced that under oscillatory flow and waves propagating over slopes or breaking, values existing in the literature may not be valid since the experimental conditions for obtaining those formulae were not considering these effects. Since there is not a predictive methodology to determine α and β coefficients in advance, calibration has to be performed.

Model calibration is carried out based on measured data from one single test for each porous material (crushed stones and glass beads), comparing computed and measured time evolution of free surface displacement at the whole fish tank including the porous dam. The middle initial water elevation case (25 cm) was considered for both granular material characteristics.

Porous flow parameters	Tested values
Linear friction parameter α	1000, 5000,10000
Nonlinear friction parameters β	0.5, 3, 6

Table 1: Tested values for the linear and nonlinear friction coefficients.

Tested values for the porous flow parameters are presented in table 1. Linear drag parameter (α) influence is studied first keeping constant the non-linear drag parameter (β) and equal to 6. Figure 3 shows the comparisons between the laboratory data and three numerical simulations performed varying the α parameter for flow passing through the crushed stones. Laboratory data are presented in circles. The linear drag parameter (α) is presented by lines. Dashed lines correspond to α= 1000, solid lines to α= 5000 and dotted lines to α= 10000. Numerical simulations are represented at the middle of the fish tank.

The three presented numerical simulations show a similar behavior, especially from t=0.0 s to t= 0.6 s when the water reservoir is released. Water motion within the porous dam is not very well predicted. In our opinion this discrepancies are due to the fact that water is released in a different way. In the numerical modeling, water is at rest at the initial stage and an instantaneous opening of the gate is considered. However in the laboratory experiments, a manually opened gate is move upwards with an estimated

time of 0.1 s[14]. The water is then first accelerated at the bottom yielding a different flow behavior at early stages. Water starts to flow from the bottom while the gate is opened.

For later stages, flow is very well predicted by the model especially for α= 5000 simulation not only within the porous dam but also at both sides. Linear drag influence is noticed when the water on the right side of the dam is calm down and the water on the left side continues to seep into the clear fluid region (see figure 3). A larger α parameter (10000) exhibits a larger drag as expected, delaying water level drop at the right side of the dam. Flow is percolating faster for the smaller α parameter (1000).

Non linear drag parameter (β) influence is studied next. Linear drag parameter (α) is kept constant and equal to 5000. Figure 4 shows the comparisons between the laboratory data and the numerical simulations for flow passing through the crushed stones. Laboratory data are presented in circles. Non-linear drag parameter (β) is presented by lines. Dotted line correspond to β= 0.5, dashed line to β= 3 and solid line to β= 6.

In this case, larger discrepancies among the three performed simulations are observed. Poor correlations can be found for β= 0.5 and 3 for time stages larger than 0.6 s. Early time stages are not considered in this analysis because of the previously commented reason. Both simulations exhibit a lower drag than expected from the experiments. Water is seeping faster into the porous dam at the right side of the tank. Water oscillations at both sides of the dam appear also different from the experiments for that parameter values. However, β= 6 simulation shows the best agreement. Larger β values (not shown here) yield larger drag and consequently a worst agreement.

Numerical simulations have also been performed for the glass bead experiments. Since glass bead characteristics (porosity and nominal diameter) differ from the crushed stones, flow within the porous dam will be different and coefficients need to be modified. A similar procedure has been carried out leading a best-fit pair for the linear (α) and the non-linear (β) drag parameters (α=700 and β=0.5). Comparisons between numerical simulations and laboratory data for the mentioned simulation are presented in figure 5. Numerical simulations (not shown here) have shown more sensitive to variations of α than for β due to the flow characteristics within the porous media, with lower Reynolds number.

As can be seen in the figure, the model accurately reproduces the free surface time history at each of the considered situations except for t=0.40 s and t=0.80 s at the toe of the percolating bore within the porous dam. Here again, the early stages are influenced by the opening gate procedure. Moreover, because the seepage process is slower due to the glass bed characteristics, the influence is also noticeable to later stages. For the rest of the presented panels, the model deals very well with the free surface evolution. Water surface levels show no significant differences either at both sides of the porous dam or within the porous obstacle.

As a conclusion, the computed and measured free surface time evolution agree very well for the two porous media tested. Porous flow parameters have been found to be different as expected because of the different flow developed at both situations. In the first case (crushed stones) due to a larger nominal diameter, a larger Reynolds number

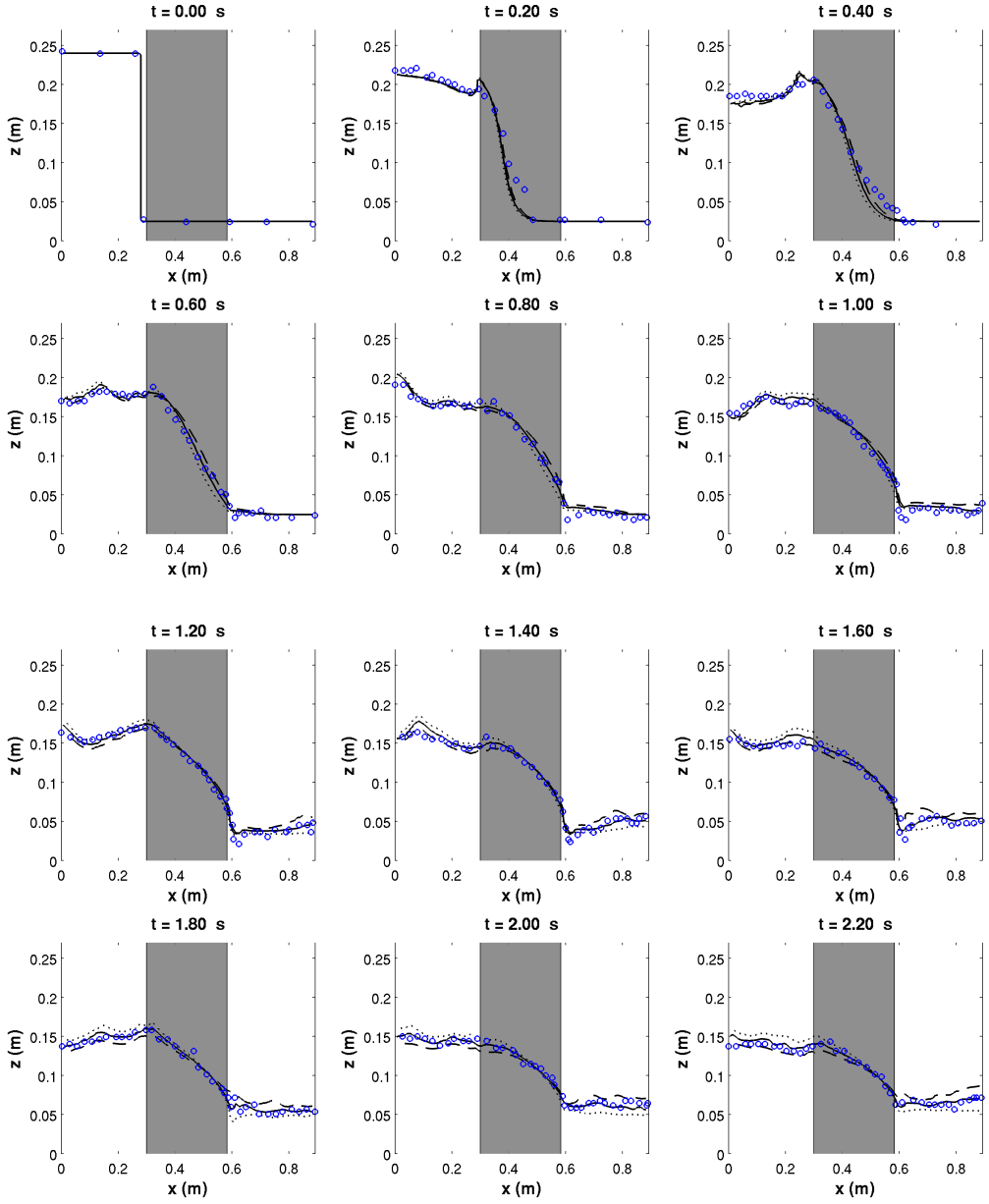

Figure 3: Linear drag parameter (α) calibration for crushed stones. Time intervals from t=0 s to t=2.20 s. Laboratory data are presented in circles. Numerical simulations for linear drag parameter (α): 1000 (dashed line), 5000 (solid line) and 10000 (dotted line).

is observed. The non-linear parameter appears as the most important parameter in the dam breaking percolating flow. For the glass bead case, linear drag parameter has the

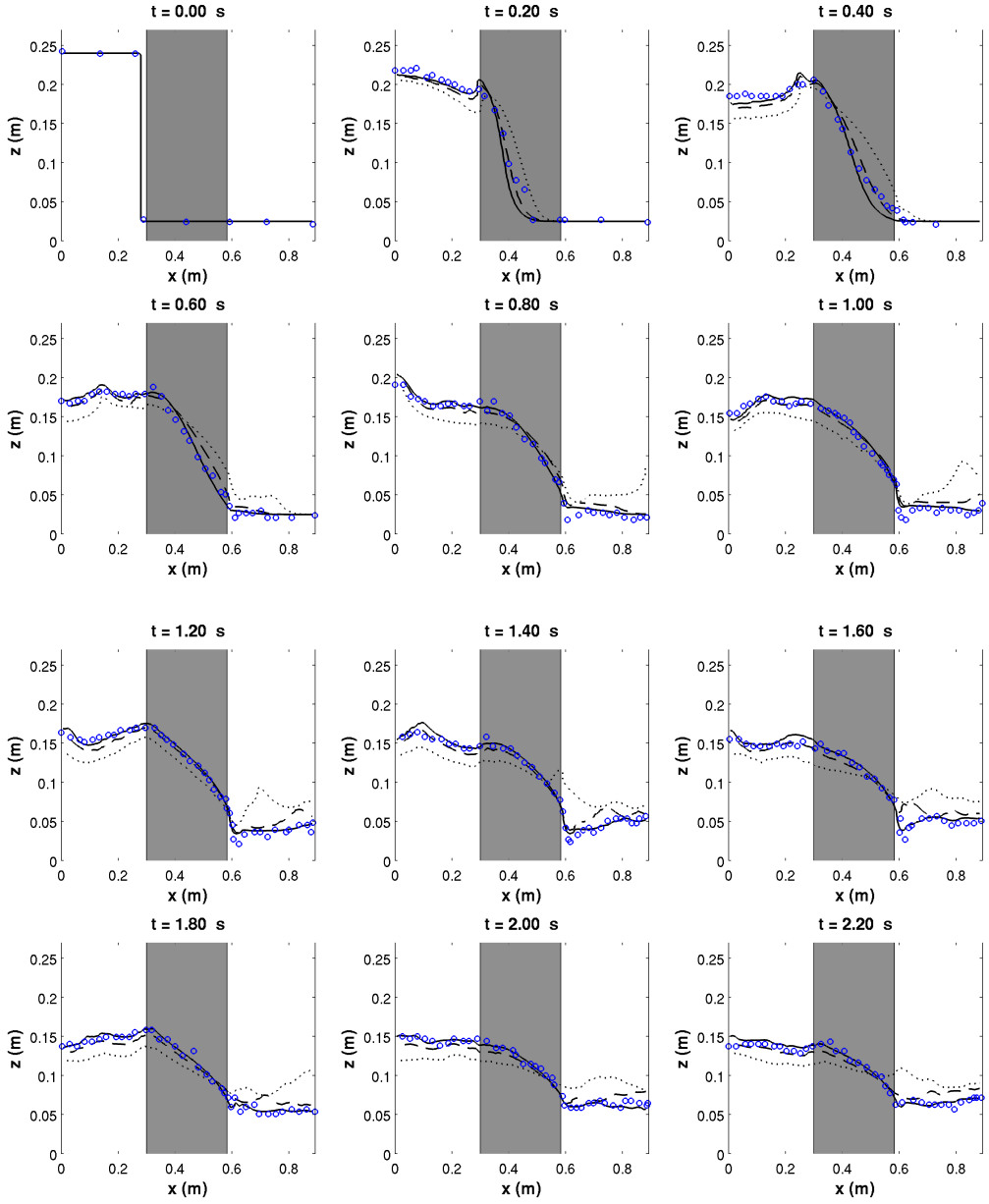

Figure 4: Non-linear drag parameter (β) calibration for crushed stones. Time intervals from t=0 s to t=2.20 s. Laboratory data are presented in circles. Numerical simulations for non-linear drag parameter (β): 0.5 (dotted line), 3 (dashed line) and 6 (solid line).

largest influence in the flow drag because the Reynolds number decreases.

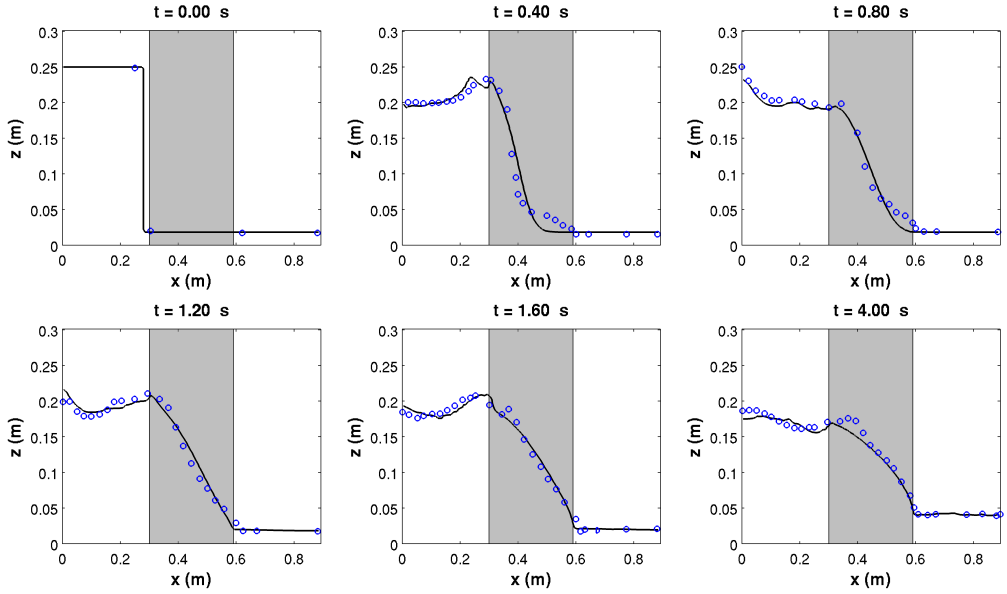

Figure 5: Calibration for glass beads: laboratory data (circles), numerical simulation (solid line).

4 Wave induced hydrodynamics

In order to validate the model behavior under the action of surface gravity waves, a specific numerical experiment has been carried out. This experiment has taken place in a numerical wave flume 24.05 m long, 0.60 m wide and 0.80 m high.

An impermeable box was placed in the wave flume 12 m far from the numerical wave paddle. It was design to do not fill the whole flume width in order to induce a three dimensional flow structure with a diffraction region and also to be overtopped. The box was 25.2 cm long, 26.1 m high and 26.1 cm wide and it was fixed to one of the side wall of the flume. A gap of 32.4 cm was set between the box and the front side wall.

Three solitary waves were generated, 5, 7 and 10 cm, on a 0.25 m water depth. In all the cases, wave overtopped the box.

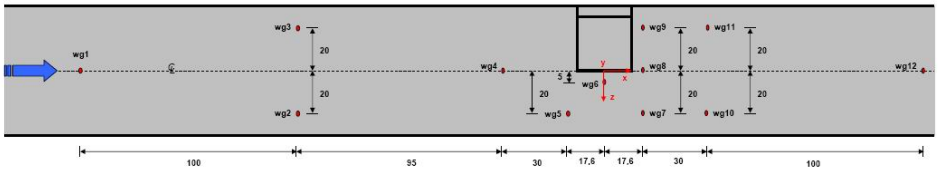

Figure 6: Description of the numerical flume geometry

The whole numerical flume has been discretized by means of a regular orthogonal mesh. The cell size was 2x2x1 cm (Δx/Δy/Δz).

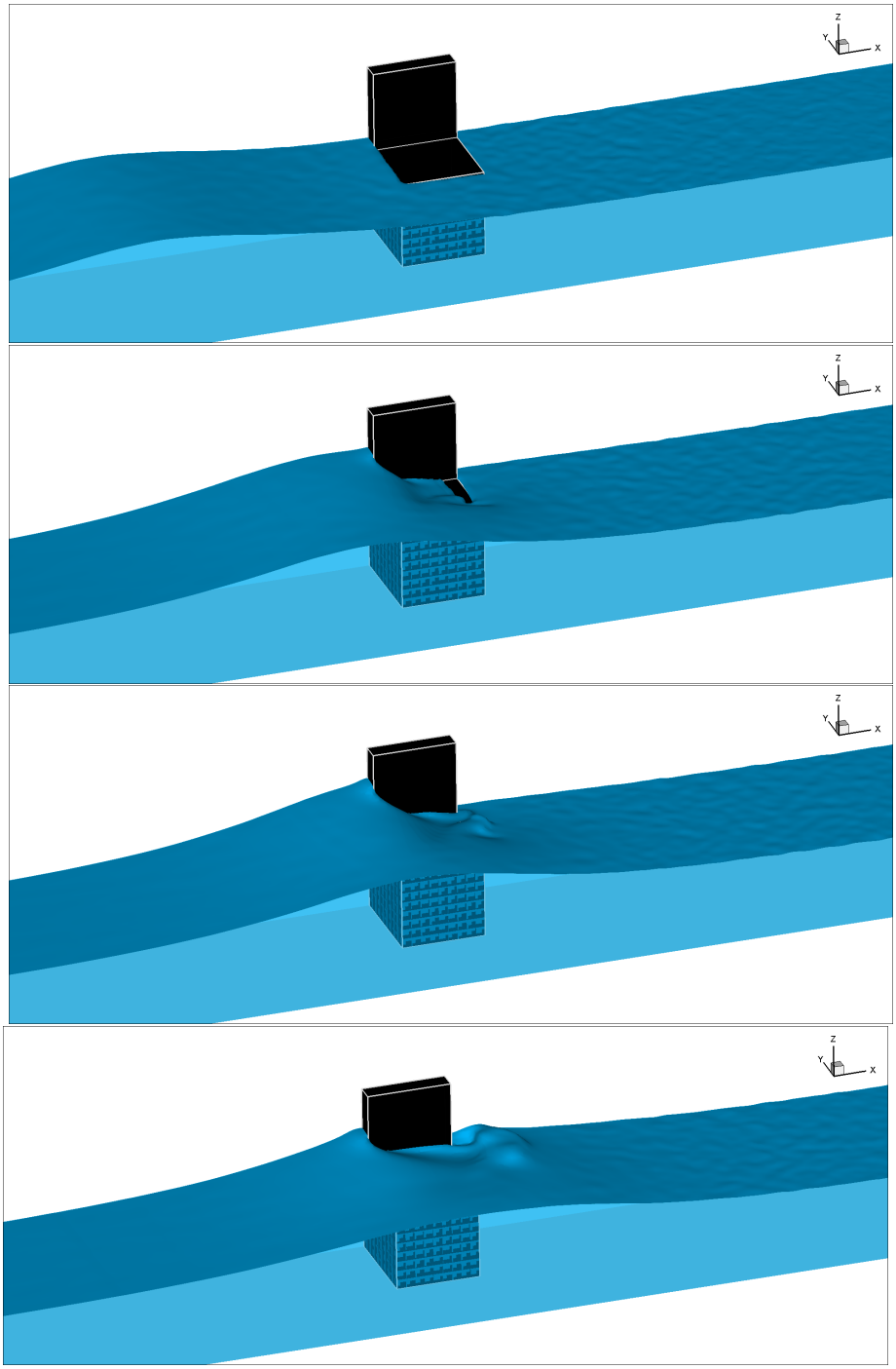

Figure 7: Snapshots of solitary wave interaction with a vertical structure.

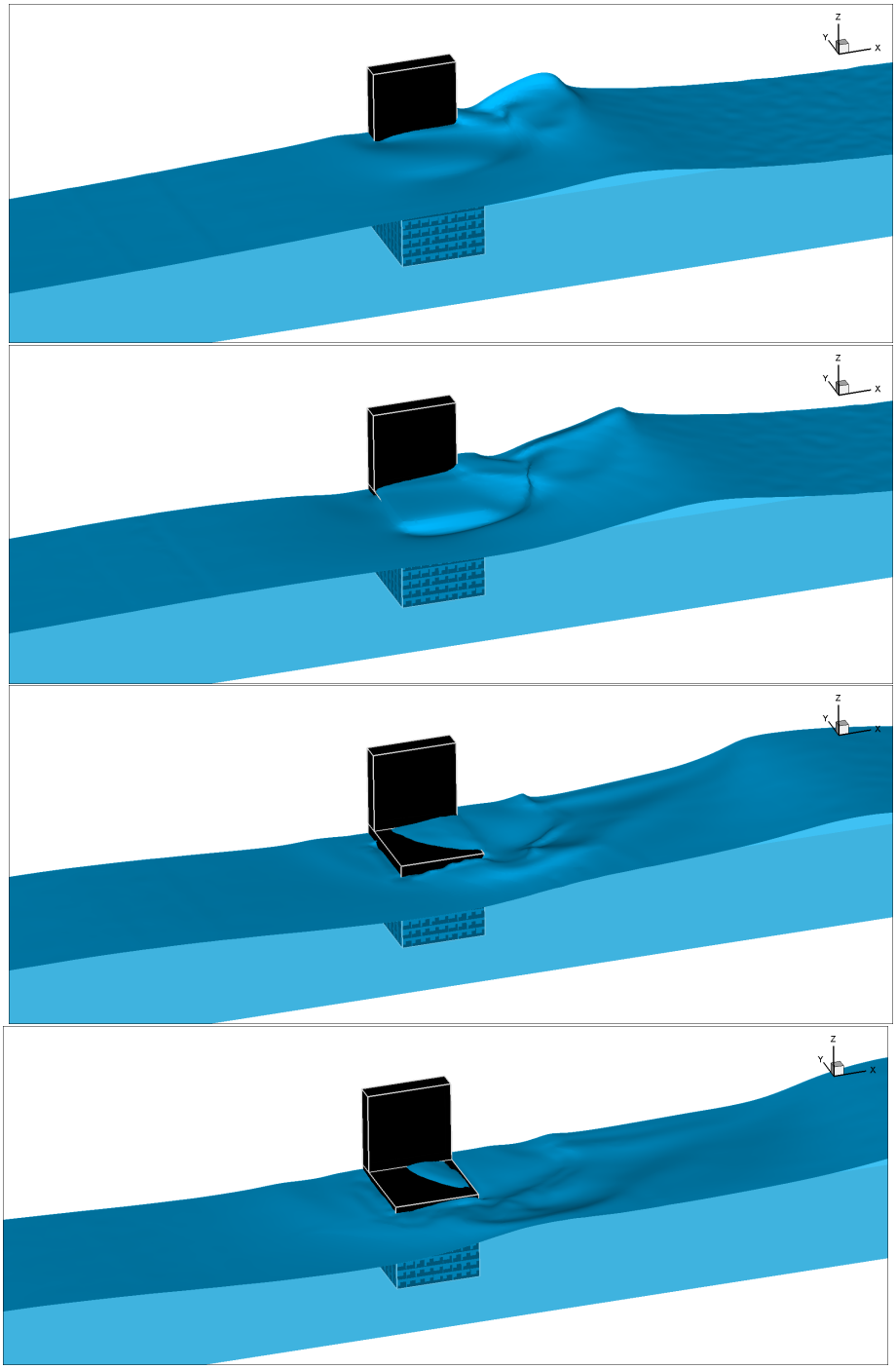

Figure 8: Snapshots of solitary wave interaction with a vertical structure.

In figures 7 and 8 several snapshots of the simulated 0.05m high solitary wave inter-

action with the structure are presented. Figure 7 shows four stages of the wave reaching the structure and overtopping the box. Part of the wave freely travels along the gap existing between the box and the flume side wall and the other part of the wave is partially reflected at the wall. A three dimensional free surface field is generated because the presence of the obstacle. Water wave breaks at the top of the box, as can be seen in the lower panel in figure 7. Once the wave crest has past along the structure, three dimensional wave patterns are observed (figure 8). Water is rushing down from the box and is reflected at both flume walls. A diffraction pattern is also visible in the second panel in figure 8, generated leeward the box.

5 Conclusions

In this paper, a three dimensional Navier-Stokes model, called IH-3VOF is presented. The model is able to deal with physical processes associated with wave-interaction with porous structures. A new set of porous flow equations are presented. A k-ϵ model was also considered in the equations, not only for the clear fluid region but also for the porous media flow.

A series of laboratory experiments of dam-break flow were used in order to calibrate and validate the model. Model calibration is carried out based on measured data from one single test for each porous material (crushed stones and glass beads), comparing computed and measured time evolution of free surface displacement at fish tank including the porous dam. Numerical simulations were calibrated by adjusting the porous flow empirical coefficients for two granular material characteristics. The model is proven to reproduce with a high degree of agreement the free surface evolution during the seeping process. Porous flow parameters have been found different for both materials as expected because the difference in the Reynolds number.

Further numerical capabilities have been shown considering solitary wave interaction with an overtopped structure. The model is able to reproduce the most relevant processes.

IH-3VOF is proven to be a powerful tool in examining the near-field flow characteristics around porous structures. Numerical information can be used to study physical magnitudes difficult or impossible to measure in the laboratory, such as particle velocity above or around the structures in wave breaking conditions or flow inside the porous media.

The numerical modelling based on RANS or Large Eddy Simulation (LES) is a breakthrough in our future way of approaching coastal structures design and it is currently in a relative early but solid stage. Additional work is still to be done in order to carry out a reliable use of these models for engineering design.

6 Acknowledgments

This work is partially funded by the projects BIA2008-05462 and CT2008-06044 from the spanish Ministerio de Ciencia e Innovación. J.L. Lara is indebted to the Ministerio de Ciencia e Innovación for the funding provided in the Ramon y Cajal Program. M. del Jesus is indebted to the Ministerio de Ciencia e Innovación for the funding provided in the F.P.U Program.

REFERENCES

[1] N. Kobayashi and A. Wurjanto, Wave transmission over submerged breakwaters, *Journal of Waterways Port, Coastal and Ocean Engineering* **115**, pp. 662680 (1989)

[2] N. Kobayashi, A. Farhadzadeh, and J. A. Melby, Wave Overtopping and Damage Progression of Stone Armor Layer, *Journal of Waterway, Port, Coastal, and Ocean Engineering*, In Press

[3] J.T. Kirby, Boussinesq models and applications to nearshore wave propagation, surf-zone processes and wave-induced currents. *V.C. Lakhan, Editor, Advances in Coastal Modelling, Elsevier*, pp. 141 (2003)

[4] P. J. Lynett, P. L.-F. Liu, I. J. Losada, and C. Vidal, Solitary Wave Interaction with Porous Breakwaters, *Journal of Waterway, Port, Coastal, and Ocean Engineering*, **126** (6), pp. 314-322 (2000)

[5] I.J. Losada, J.L. Lara, R. Guanche and J.M. Gonzalez-Ondina, Numerical analysis of wave overtopping of rubble mound breakwaters, *Coastal Engineering* **55** (1), pp. 4762 (2008)

[6] J.L. Lara, I.J. Losada and R. Guanche, Wave interaction with low mound breakwaters using a RANS model, *Ocean engineering*, **35**, pp. 13881400 (2008)

[7] R. Guanche, I.J. Losada and J.L. Lara. Numerical analysis of wave loads for coastal structure stability, *Ocean engineering*, **56**, pp. 543-558 (2009)

[8] S. Shao. Incompressible SPH flow model for wave interactions with porous media, *Coastal Engineering* **57** (3), pp. 304-316 (2010)

[9] Dongming Liu, Pengzhi Lin. Three-dimensional liquid sloshing in a tank with baffles, *Ocean engineering*, textbf36, (2), pp. 202-212 (2009)

[10] Z. Wang, Q. Zou and D. Reevea. Simulation of spilling breaking waves using a two phase flow CFD model, *Computers & Fluids*, **38**, (10), pp. 1995-2005 (2009)

[11] Erik Damgaard Christensen, Large eddy simulation of spilling and plunging breakers, *Coastal Engineering*, **53**, (5-6), pp. 463-485 (2008)

[12] T. Li, P. Troch and J. De Rouck, Wave overtopping over a sea dike, *Journal of Computational Physics* **198** (2), pp. 686726 (2004)

[13] W.J. Rider and D.B. Kothe. Reconstructing volume tracking, *Journal of Computational Physics* **141** (2), pp. 112-152 (1998)

[14] Lin, P., Numerical modeling of breaking waves, *PhD thesis. Cornell University*, (1998)

[15] T.-J. Hsu, T. Sakakiyama and P.L.-F. Liu, A numerical model for wave motions and turbulence flows in front of a composite breakwater, *Coastal Engineering* **46**, pp. 2550 (2002)

[16] M.R.A. Van Gent, Porous flow through rubble-mound material, *Journal of Waterway Port, Coastal and Ocean Engineering* **121**, pp. 176181 (1995)

[17] H.F. Burcharth and O.H. Andersen, On the one-dimensional steady and unsteady porous flow equations, *Coastal Engineering* **24**, pp. 233257 (1995)

[18] N. Garcia, J.L. Lara and I.J. Losada, 2-D numerical analysis of near-field flow at low-crested permeable breakwaters, *Coastal Engineering* **51**, pp. 9911020 (2004)

[19] J.L. Lara, N. Garcia and I.J. Losada, RANS modelling applied to random wave interaction with submerged permeable structures, *Coastal Engineering* **53**, pp. 395417 (2006)

[20] J.L. Lara, I.J. Losada and P.L.-F. Liu, Breaking waves over a mild gravel slope: experimental and numerical analysis, *Journal of Geophysical Research*, **AGU 111**, p. C11019 (2006)

[21] A. Nakayama and F. Kuwahara. A macroscopic turbulence model for flow in a porous medium, *Journal of fluids engineering*, **121**, pp.427-433 (1999)